Tetrahedron 66 (2010) 5566–5572

Contents lists available at ScienceDirect

Tetrahedron

journal homepage: www.elsevier.com/locate/tet

Synthesis of 3,5-diazabicyclo [5.1.0] octenes. A new platform to mimic glycosidase transition states

Fedra M. Leonik [b], Ion Ghiviriga [a], Nicole A. Horenstein [a,*]

[a] Department of Chemistry, Box 117200, University of Florida, Gainesville, FL 32611-7200, USA
[b] Adesis, Inc. 27 McCullough Drive, New Castle, DE 19720, USA

ARTICLE INFO

Article history:
Received 16 March 2010
Received in revised form 15 May 2010
Accepted 17 May 2010
Available online 11 June 2010

ABSTRACT

All-*cis* 1-hydroxymethyl 2,3 bis-aminomethyl cyclopropane was used to construct the first 3,5-diazabicyclo [5.1.0]-3-octenes. This system has the interesting ability to exist in a conformation that resembles a snapshot of a glycoside hydrolysis reaction with respect to charge and geometric analogy to an oxocarbenium ion, and the positioning of the departing aglycon. The *cis*-configured cyclopropane core was synthesized by Cu-catalyzed intramolecular cyclopropanation of benzyl protected *cis*-2-butene-1,4-diol diazoacetate ester. Serial functionalization to bis-aminomethyl cyclopropanes and subsequent cyclization to amidines lead to the target bicyclic compounds in good overall yields. Several glycosidases were surveyed for the inhibitory potential of these transition state analogs, and amongst them, selective competitive inhibitors with micromolar K_i values were identified.

1. Introduction

As an enzyme guides reacting substrate ensembles over the reaction coordinate, it provides a dynamic complementarity to afford low energy pathways leading to products.[1,2] A significant component to the rate acceleration has been ascribed to transition state complementarity,[3] whereby favorable binding interactions between enzyme and the fleeting transition state provide a decrease in the activation barrier. As this concept evolved further, the observed tight binding of stable chemical compounds that were analogs of the transition state was rationalized on the basis of the favorable complementarity between the transition state analog and the enzyme.[4] A number of potent inhibitors has been identified that presumably operate in this way.[5–7] This is never a simple matter; an implicit design problem is that stable ground state molecules only approximate the electronic and geometric configuration of a transition state. For example, consider S_N2-like (e.g., A_ND_N type)[8] reactions, there is a degree of pentavalent character at the electrophilic carbon that depends on nucleophile and leaving group bond orders, and the timing, or symmetry of bond breaking and formation. Likewise, in a dissassociative S_N1-like e.g., $[D_N+A_N]$[8] reaction that generates carbocationic transition states or intermediates, (or the corresponding capture of these species by nucleophile in the reverse reaction) the leaving group departs in a trajectory nearly orthogonal to the plane defining the carbocation atoms (Fig. 1).

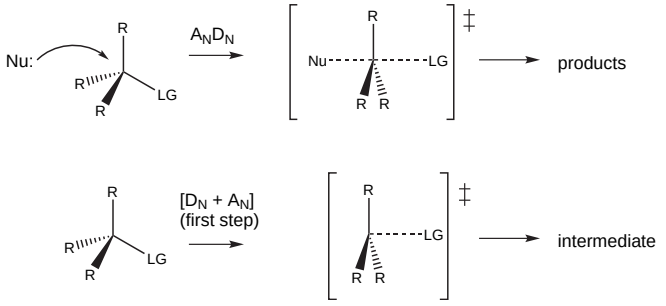

Figure 1. Transition structures for hypothetical associative and disassociative reactions. Note the non-standard geometries at the central carbon atom.

In both of these reaction types, the bonding between the leaving group, nucleophile, and central carbon atom have non-ground state angular geometries and partial bonds having lengths greater than found for stable ground state molecules. Mimicry of these structures using direct connectivity with first or second row elements is difficult, if not impossible. We sought to develop an approach to circumvent the geometric limitations imposed by direct connectivity. Our initial focus is on glycosidase and

* Corresponding author. Tel.: +1 352 392 9859; e-mail address: horen@chem.ufl.edu (N.A. Horenstein).

0040-4020/$ – see front matter © 2010 Elsevier Ltd. All rights reserved.
doi:10.1016/j.tet.2010.05.064

glycosyltransferase enzymes, responsible for creation of carbohydrate structures of incredible diversity and complexity.[9] The creation and hydrolysis of the glycosidic bond are central to the extremely broad biological functions found for carbohydrates,[10] making glycosyl transfer enzymes important targets for inhibition.[11] The reaction mechanisms for glycosidases vary in detail with respect to acid/base chemistry, and the nature of nucleophilic participation.[12,13] However, with few exceptions[14] a common mechanistic element is that as the glycosidic bond is being cleaved, the sugar glycon develops oxocarbenium ion character. This places the departing aglycon in a Burgi/Dunitz like trajectory[15,16] over the glycon ring, which is flattened and positively charged.[17,18] Figure 2 shows a conceptual model for inhibitor design whereby the transition state is simulated with a rigid bicyclic ring system used to position an aglycon analog over the plane of a positively charged ring, analogous to the flattened oxocarbenium ion like transition state of typical glycohydrolase enzymes.

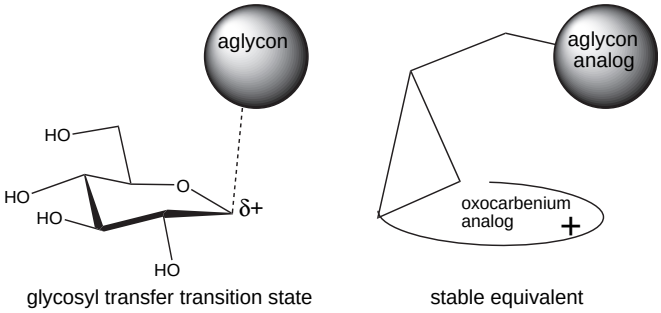

Figure 2. A mimic (right) for disassociative glycosyl transfer transition states (left).

With the exploration of this design strategy, we expand the well-known ability of sugar analogs with basic nitrogen atoms to inhibit glycosidases.[7,19,20] Further, inclusion of the aglycon or a nucleophile into the inhibitor structure with transition state geometric constraint affords opportunities to increase binding affinity and direct specificity. In the present study, we describe synthesis of parent molecules that could serve to validate this concept and provide the basis for synthesis of more elaborate compounds. Figure 3 presents our targets, substituted 3,5-diazabicyclo-[5.1.0] octanes, which to the best of our knowledge have not been reported. They are both geometric and charged analogs of glycosidase transition states. The amidinium portion of the ring mimics the charge and shape of a glycosyl oxocarbenium ion,[21] because it is flattened, positively charged, and has delocalization of charge. The all-*cis* cyclopropyl ring system creates an oriented tether with

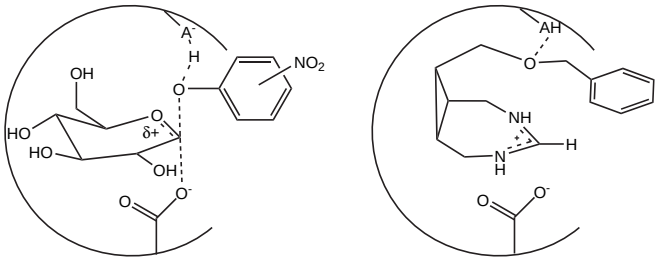

Figure 3. Archetypical glycosidase transition state and bicyclic amidinium analog. On the left is a model for an enzyme bound glycosidase transition state featuring oxocarbenium ion character and the leaving group orthogonal to the π-system of the oxocarbenium ion. The bicyclic amidine on the right places an analog of a phenolic leaving group aglycon above the amidine plane that mimics the electronics and flat geometry of an oxocarbenium ion.

which to attach an analog of a leaving group aglycon. Earlier work has explored geometric and electronic aspects of this design.[22,23] The compounds we report here are an interesting counterpoint to the calystegines, which are glycosidase inhibitors with a bridged bicyclic nortropane skeleton.[24] Presumably the bicyclic framework of the calystegines serves to rigidify the ring and hydroxyl group positions, whereas, the design presented in this work utilizes a bicyclic diaza-framework to position the aglycon and provide delocalized charge mimicry.

2. Results and discussion

2.1. Synthesis of bicyclic amidines

We envisioned arriving at our target [5.1.0] diaza bicyclooctenes by cyclization of bis-amino all-*cis* cyclopropanes. Scheme 1 presents the route for synthesis of the key intermediate bis-aminomethyl cyclopropane **8**.

cis-2-Butene-1,4-diol **1** was converted to the monobenzylated derivative **2** using standard methods.[25] Subsequent reaction of the free hydroxyl group with diketene gave the unsaturated β-keto ester **3** in 86% yield.[26] Reaction of **3** with *p*-ABSA (*p*-acetamido benzenesulfonyl azide) in Et_3N gave the desired *cis*-diazoacetic ester **4**.[26] A key step in this synthetic design was the intramolecular cyclopropanation of **4** to give an all-*cis* trisubstituted cyclic system. With intramolecular cycloaddition, only one fused bicyclic ring is formed due to geometric constraints.[27] Hence, starting from a *cis*-alkene, the resulting fused cyclopropyl lactone **5**[26] will have all substituents in an all-*cis* relative configuration. Several cyclopropanation catalyst systems were explored, leading to identification of copper triflate and Evan's bis-oxazoline valinol ligand[28] as being optimal, producing (+)-**5** in 60% yield. The ee obtained for **5** was only 22%,[26] but was fully acceptable for this work given that our target and intermediates were *meso* compounds. The lactone ring of **5** was reductively opened with $LiAlH_4$ to give the *meso* diol **6** in 74% yield. Conversion to the bis-azide **7** was smoothly effected by mesylation of **6** and displacement with azide in DMF at 60 °C. The diazide **7** was used without further purification for synthesis of diamine **8** in (95% yield, two steps) by triphenylphosphine mediated reduction. All-*cis* cyclopropanes related to compound **8** have recently been discussed as potential tripodal ligands for Pd-based catalysts, so compounds like **8** may be of further interest for creation of new Pd ligands.[29]

Scheme 2 presents the conversion of **8** into different bicyclic amidines **9**–**13**. Initial attempts to synthesize compound **9** using neat trimethyl orthoformate/HCl instead lead to bis-formamide **14** based on MS and 500 MHz NMR analyses. While cyclization with 1 equiv of trimethyl orthoformate proved to afford **9** in 46% yield, we sought an alternate method to give improved yields. Reaction

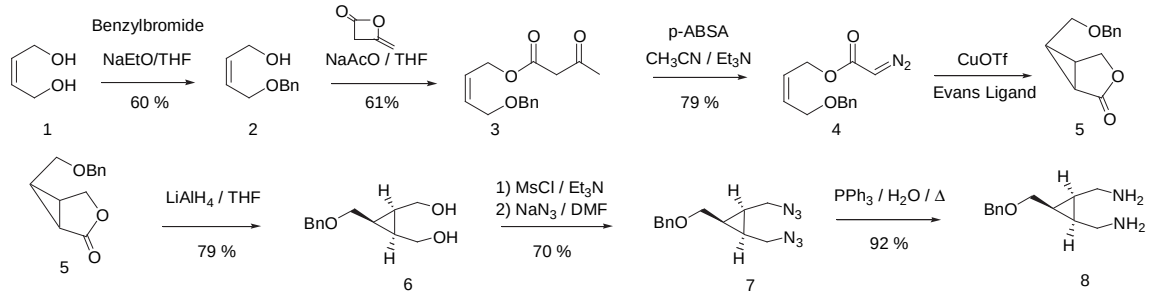

Scheme 1. Synthesis of bis-aminomethyl cyclopropane **8**.

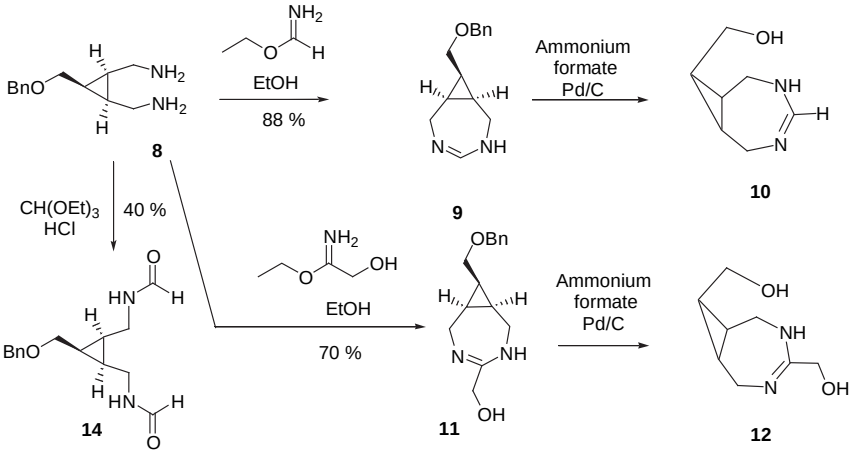

Scheme 2. Synthetic route to the [5.1.0] diaza bicyclooctenes.

of **8** with the appropriate imidate ester hydrochloride[30] in refluxing absolute ethanol lead to bicyclic amidines **9** and **11** in 88% and 70% yields, respectively. The relative stereochemistry of amidine **9** was analyzed by NOESY 2D NMR in order to confirm the all-*cis* configuration. A strong cross peak was observed between H_a (3.70 ppm) and H_b (3.93 ppm), confirming the stereochemistry we anticipated based on intramolecular cyclopropanation of *cis*-butene **4**.

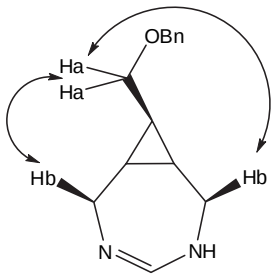

Hydroxymethyl amidine **10**, and bis-hydroxymethyl amidine **12** were synthesized by catalytic transfer hydrogenation of compounds **9** and **11**, respectively, giving in both cases quantitative conversion. The new amidines were found to be stable in aqueous solution near neutral pH for at least 24 h, based on NMR analyses. Another point about the bicyclic amidines is that although they are racemic in their neutral form, they are protonated in aqueous media (see enzymology below) and are therefore *meso* compounds in water at neutral pH.

A molecular mechanics conformational analysis of compound **9** was performed to investigate the overall ring conformation and the disposition of the benzyl group with respect to it. The *exo*,*exo* conformer shown in Figure 4 was the global minimum based on a search through rotational itinerary of all C–C non ring bonds and alternate ring puckers on the seven-membered portion of the [5.1.0] system. The *exo*,*exo* designation refers to the *exo*-ring pucker and the *exo*-disposition of the benzyl group with respect to the fused ring system. The transition-state like *endo*,*endo* conformer was a local minimum, estimated to be 2.2 kcal/mol higher in energy than the *exo*,*exo* conformer. While it suffers from a modestly higher angle strain term, **9**-*endo*,*endo* does enjoy a favorable dipole/charge term that we ascribe to the non-bonding electrons of the benzyl oxygen and the positive charge of the amidinium moiety given their close proximity. We suggest that **9**-*endo*,*endo* is an energetically accessible conformation, relevant for enzymatic binding. Effective enzymatic recognition does not require that the global minimum in solution be the bound species, especially when energetically close local minima may bind with interactions that offset a small solution penalty.[31]

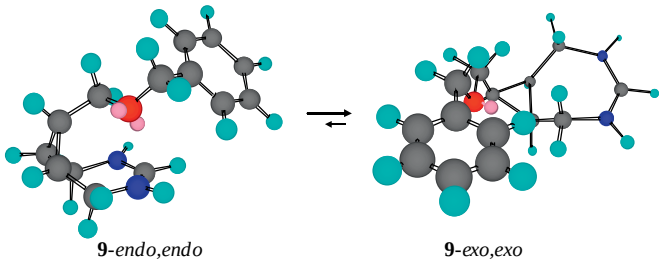

Figure 4. The transition state like conformation and global minimum for compound **9** via molecular mechanics.

2.2. Inhibition of glycosidases

The bicyclic amidines **9**–**12** were screened against a small panel of α- and β-glycosidases to yield the data reported in Table 1. All of the glycosidases utilized in these experiments were retaining enzymes, and the appropriate *p*-nitrophenyl (PNP)-glycosides were used as substrates. The inhibition screening data are presented as percentage inhibition, as expressed by Eq. 1, where v_0 is the initial velocity in the absence of inhibitor, v_i is the initial velocity in the presence of inhibitor.

$$\%\ \text{inhibition} = (v_0 - v_i)/v_0 \times 100 \quad (1)$$

Table 1
Inhibition screens for compounds **9**–**12**

Compound	α-Galactosidase from green coffee beans (%)		α-Glucosidase from *S. cerevisiae* (%)		β-Galactosidase from *A. orizae* (%)		β-Galactosidase from *E. coli* (%)		β-Glucosidase from almonds (%)	
	pH 7.5	pH 6	pH 7.5	pH 6	pH 7.5	pH 6	pH 7.5	pH 6	pH 7.5	pH 6
9	2	—	—	—	16	16	10	—	83	65
10	—	4	2	—	11	—	3	—	45	24
11	2	—	—	3	40	16	10	13	87	71
12	—	3	—	—	34	—	10	5	46	26

The data are expressed as % inhibition, as defined in the text. A dash (—) indicates no inhibition was observed.

In the experiments the concentration of substrate and inhibitor were both set to the substrate K_m, which would give a reasonably sensitive probe for effective inhibition.

The screening data of Table 1 demonstrate that α-galactosidase and α-glucosidase were not inhibited significantly by any of the compounds. Table 1 also reveals that almond β-glucosidase was inhibited to varying degree by all of the compounds, which is in accord with its broad specificity.[32] However, the data presented in Table 1 also suggest that β-glucosidase inhibition is promoted by inclusion of aglycon mimicry in the amidine inhibitors. Comparison of inhibition data for **9** versus **10**, and **11** versus **12**, shows a halving of the apparent inhibition when the benzyl functionality is absent. From the comparison between molecules **9** and **11**, it was observed that including a hydroxyl group doubled the potency of the amidines TS analog, indicating a modest contribution to binding.

One general trend seen in the data for almond β-glucosidase is that the inhibition appears to be stronger at pH 7.5 than at pH 6.0. This is unlikely to be a reflection of an unusually low amidine pK_a, because our titrametric estimate of the pK_as for **9** and **11** placed them over 10.0. It is possible that the pH behavior observed here reflects a deprotonated state of the enzyme with better electrostatics for binding the amidines at higher pH. A deeper investigation and interpretation of the pH behavior will be of interest, but is beyond the scope of the present study. As most recently discussed by Davies, analysis of glycosidase inhibitor binding is exceptionally complex, impacted in varying ways by enthalpic and entropic factors.[33]

The three β-glycosidases tested showed diverse responses to compounds **9**–**12** under screening conditions, enabling identification of enzyme/inhibitor combinations for characterization. Compounds **11** and **12** were selected for further kinetic analysis with the β-galactosidase from *Aspergillus oryzae* and compounds **9** and **11** were selected for analysis with almond β-glucosidase. In those experiments, initial velocity measurements were obtained over a range of substrate and inhibitor concentrations, and the data were found to be well-fit to the equation for competitive inhibition. The estimated K_i values and K_m/K_i ratios are presented in Table 2.

The double reciprocal plot for the inhibition kinetics of compound **11** with β-glucosidase from almonds is presented in Figure 5.

Table 2
Inhibition constants, K_i, μM, and K_m/K_i for compounds **9**, **11**, **12** at pH 7.5

Compound	β-gal/*A. orizae* K_i; K_m/K_i	β-glc/almond K_i; K_m/K_i
9	nd	270±40; 18
11	760±90; 2.1	150±30; 32
12	1500±100; 1.1	nd

nd=not determined

The estimated K_i for **11** is 150±30 μM, and the inhibition mode is competitive. Removing the hydroxymethyl group (compound **9**, K_i=270±40 μM) or the benzyl aglycon mimic (compound **12**) results in decreased inhibition.(Tables 1 and 2) The 2-fold higher K_i for **9** versus **11** for almond β-glucosidase suggests that the hydroxymethyl group of **11** engages in an active site hydrogen bond, the nature of which remains to be determined. Inhibition of almond β-glucosidase was facilitated when compounds included a benzylic group analogous to the departing aglycon of the PNP substrate as evidenced by the data for compound **11** versus **10** or **12**.

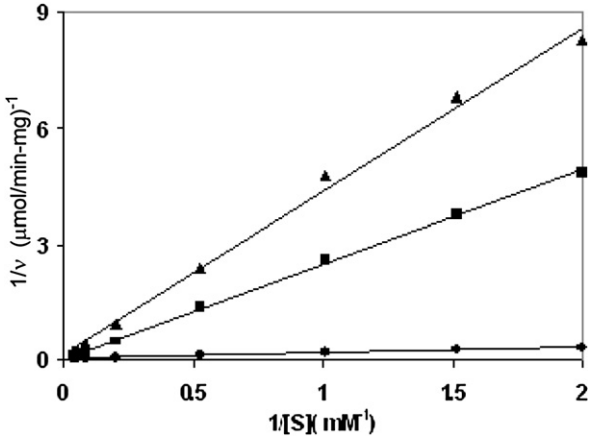

Figure 5. Lineweaver/Burk plot for almond β-glucosidase with β-PNP-glucoside as substrate and compound **11** at concentrations of: ▲, 4 mM; ■, 2 mM; •, 0 mM. K_i=150±30 μM.

The trends observed in the inhibition data for the *A. orizae* β-galactosidase parallel those for the almond β-glucosidase. In particular, compound **11** is the best inhibitor, with a K_i of 760±90 μM, and loss of the hydroxymethyl or benzylic functionalities (K_i=1,500±100 μM) results in poorer binding interactions.

3. Conclusions

We have described the first syntheses of diazabicyclo [5.1.0] octenes with an all-cis configuration about the cyclopropyl ring and an overall *endo* configuration for the system. This ring system has been used to develop a prototype glycosidase inhibitor design in

which the planar amidine functionality serves as an electronic and geometric mimic of a glycosyl oxocarbenium ion. The overall *endo* configuration allows incorporation of leaving group (aglycon) mimicry into the molecule, but importantly, allows it to assume a position over the amidine group that mimics the hypervalent shape and trajectory a departing aglycon enjoys relative to the flattened oxocarbenium ion-like glycon. We have identified selective inhibition of two beta glycosidases. The best K_i was 150 μM, for compound **11** against almond β-glucosidase, with a corresponding K_m/K_i ratio of 32. What is notable about the 32-fold binding advantage for competitive inhibitor **11** is that effective micromolar inhibition has been obtained with an austere substitution pattern lacking the hydroxylation, that is, found in the substrate, or found in the 200 μM competitive inhibitor gluconolactone.[32] We hypothesize that inclusion of an appropriate hydroxylation pattern about the bicyclic ring system will result in opportunities to lower K_i values and provide the platform for in-depth analysis of the nature of inhibition and transition state analogy[34] in these compounds.

4. Experimental section

4.1. General

Solvents and reagents were purchased from Aldrich and Acros. Glycosidase enzymes and nitrophenyl glycoside substrates were purchased from Sigma. The organic solvents were dried overnight over CaH_2 or 4 Å molecular sieves and freshly distilled before use. NMR spectra were obtained at 300 MHz for ^1H and 75 MHz for ^{13}C, Varian spectrometers (VXR, Gemini, Mercury). Chemical shifts were referenced to internal tetramethylsilane, 0 ppm in appropriate deuterated solvents. Mass spectra were obtained on a Finnigan MAT 95Q spectrometer operated in FAB or EI modes. Infrared (IR) spectra were obtained by deposition of $CHCl_3$ solutions on NaCl plates followed by evaporation of the solvent. Optical rotations were recorded on a Perkin/Elmer 241 polarimeter at the sodium D line. UV/vis spectra were obtained with Beckman DU 640 and Agilent 8453 spectrometers. Constant temperature was maintained with an Isotemp 210 from Fisher Scientific. Molecular mechanics calculations utilized MM2 parameters as implemented within Chem3D Ultra 6.0 (CambridgeSoft.com).

*4.1.1. Z-4-Benzyloxy-but-2-en-1-ol (**2**).* The title compound was synthesized by the reported method.[25] *cis*-2-Butene 1,4-diol (56.7 ml, 690 mmol) was added to a stirred suspension of NaH (60% dispersion in mineral oil, 5.5 g, 138 mmol) in THF (460 ml) that was previously cooled to 0 °C. Stirring was continued at room temperature for 30 min. After this, benzyl bromide (14.0 ml, 118 mmol) was added. The reaction mixture was stirred at room temperature until starting material was consumed. The THF was removed by rotary evaporation and the residue was dissolved in ether (400 ml). The organic layer was washed with water (3×150 ml) and dried over $MgSO_4$. Fractional distillation of the crude product at 5 mm Hg (bp 156–159 °C; lit.[25] $97_{0.25}$ °C) gave the desired mono protected diol in 60% yield (12.9 g). ^1H NMR ($CDCl_3$) δ ppm 2.02 (br s, 2H), 4.06 (d, J=6 Hz, 2H), 4.13 (d, J=6 Hz, 2H), 4.50 (s, 2H), 5.75 (m, 2H), 7.32 (m, 5H).

*4.1.2. (Z)-4-Benzyloxy-but-2-enyl 3-oxobutanoate (**3**).* The title compound was synthesized according to published methodology.[26] Mono protected diol **2** (2.00 g, 11.2 mmol) was dissolved in 8 ml of anhydrous THF containing NaOAc (56 mg, 0.68 mmol). A solution of diketene (1.0 ml, 12.6 mmol) in 4 ml of THF was added dropwise over 1 h to the refluxing mixture. The mixture was refluxed for 1 h until complete consumption of mono protected diol was observed. The reaction mixture was taken up in ether (40 ml) and washed with brine (60 ml). The organic phase was dried over $MgSO_4$ and evaporated under vacuum. The crude oil was purified by flash chromatography (silica, 6:1 petroleum ether/AcOEt) to give **3** in 60% yield (1.80 g). ^1H NMR ($CDCl_3$) δ ppm 2.25 (s, 3H), 3.44 (s, 2H), 4.12 (d, J=8 Hz, 2H), 4.51 (s, 2H), 4.68 (d, J=8 Hz, 2H), 5.71 (m, 1H), 5.82 (m, 1H), 7.33 (m, 5H), ^{13}C NMR ($CDCl_3$) δ (ppm) 200.7, 167.3, 138.4, 131.9, 128.9, 128.2, 126.4, 73.0, 66.1, 61.6, 50.4, 30.6.

*4.1.3. Diazo-acetic acid 4-benzyloxy-but-2-enyl ester (**4**).* The title compound was synthesized using the reported procedure.[26] A solution of acetoacetate ester **3** (1.72 g, 6.56 mmol) and Et_3N (1.15 ml, 8.47 mmol) in anhydrous acetonitrile (18 ml) was prepared at room temperature. Then a solution of *p*-ABSA (2.05 g, 8.54 mmol) in acetonitrile (18 ml) was added dropwise over a 30 min period. The reaction mixture was stirred for 3 h, after which time a solution of 3 N LiOH was added and the mixture was left to stand for approximately 12 h. The reaction mixture was then extracted with ether/AcOEt 2:1 (3×50 ml). The organic layers were combined and extracted with brine (100 ml), dried over $MgSO_4$, and concentrated by rotary evaporation. The crude product was purified by flash chromatography (silica, 10:1 petroleum ether/AcOEt) to give **4** as a yellow oil in a 86% yield (1.40 g). ^1H NMR ($CDCl_3$) δ ppm 4.12 (d, J=6 Hz, 2H), 4.49(s, 2H), 4.70 (d, J=7 Hz, 2H), 4.71(br s, 1H), 5.70 (m, 1H), 5.78 (m, 1H), 7.31 (m, 5H), ^{13}C NMR ($CDCl_3$) δ (ppm) 167.0, 138.4, 131.4, 128.9, 128.3, 127.0, 72.9, 66.1, 61.0, 46.7. IR: 2116s, 1687s. EI HRMS calcd for $C_{13}H_{14}N_2O_3Na$ (MNa^+): 269.0897, found: 269.0901. The spectroscopic data were consistent with previous data.[25]

*4.1.4. (1S,5R,6S)-6-(Benzyloxymethyl)-3-oxabicyclo[3.1.0]hexan-2-one (**5**).* Diazoester **4** (3.00 g, 12.2 mmol) was dissolved in dry CH_2Cl_2 (131 ml) to make a 0.09 M solution of the starting material. This solution was added from an addition funnel to a refluxing suspension of CuOTf (61 mg, 0.25 mmol) and Evan's bis-oxazoline ligand[28](prepared as described)[35] (80 mg, 0.27 mmol) in 400 ml of CH_2Cl_2 over a period of 18 h. When the addition was finished, the solvent was removed under vacuum and the residue was purified by flash chromatography (silica, 5:1 hexanes/AcOEt). The bicyclic product was obtained as a colorless oil in 60% yield (1.60 g). ^1H NMR ($CDCl_3$) δ ppm 1.83 (m, 1H), 2.32(dd, J=6, 9 Hz, 1H), 2.39 (dd, J=6, 7 Hz, 1H), 3.42 (dd, J=9, 11 Hz, 1H), 3.70 (dd, J=6, 11 Hz, 1H), 4.24 (d, J=10 Hz, 1H), 4.41 (dd, J=6, 10 Hz, 1H), 4.50 (d, J=12 Hz, 1H), 4.57 (d, J=12 Hz, 1H), 7.35 (m, 5H), ^{13}C NMR ($CDCl_3$) δ (ppm) 174.7, 138.2, 128.9, 128.3, 73.8, 66.8, 65.1, 22.9, 21.8. EI HRMS calcd for $C_{13}H_{14}O_3$ (M^+): 218.0943, found: 218.0944. $[\alpha]_D^{20}$ +5.3 (*c* 0.55, $CHCl_3$); ee=22%.

*4.1.5. ((1R,2S,3S)-3-(Benzyloxymethyl)cyclopropane-1,2-diyl)dimethanol (**6**).* Lactone **5** (1.00 g, 4.59 mmol) was added dropwise to a suspension of $LiAlH_4$ (1.57 g, 41.3 mmol) in dry THF (46 ml) at 0 °C. After 3 h, total consumption of starting material was observed and the reaction mixture was cautiously quenched with saturated aqueous NH_4Cl. The reaction mixture was diluted with additional THF and filtered through Celite. The organic layer was separated and dried over $MgSO_4$. After evaporation of solvent, the reaction mixture was purified by flash chromatography (silica, 2:1 petroleum ether/AcOEt). Diol **6** (0.80 g) was obtained in 74% yield. ^1H NMR ($CDCl_3$) δ ppm 1.49 (m, 3H), 2.55 (br s, 2H), 3.63(m, 2H), 3.70 (m, 2H), 3.78 (m 2H), 4.54 (s, 2H), 7.34 (m, 5H), ^{13}C NMR ($CDCl_3$) δ (ppm) 138.0, 128.9, 128.4, 128.3, 73.6, 66.6, 59.2, 22.2, 19.5. EI HRMS calcd for $C_{13}H_{19}O_3$ $(M+H)^+$: 223.1334, found: 223.1330.

*4.1.6. ((((1S,2R,3S)-2,3-Bis(azidomethyl)cyclopropyl)methoxy)methyl)benzene (**7**).* A mixture of diol **6** (0.38 g, 1.7 mmol) and Et_3N (0.56 ml, 5.08 mmol) in CH_2Cl_2 (57 ml) was cooled to 0 °C. Freshly

distilled methanesulfonyl chloride was added dropwise (0.40 ml, 5.1 mmol) and the resulting mixture was stirred at 0 °C for 20 min, at which time all of the starting material was consumed. The reaction mixture was washed with water, then brine, and dried over $MgSO_4$. The crude dimesylated product was dissolved in DMF (35 ml) and NaN_3 was added. The reaction was stirred at 60 °C for 4 h and the solvent was evaporated under reduced pressure. The residue was dissolved in AcOEt (150 ml) and washed with water (3×100 ml). The organic phase was dried over $MgSO_4$ and the solvent removed by rotary evaporation. The product was purified by flash chromatography (silica, 20:1 petroleum ether/AcOEt) giving a white solid in 73% yield (0.30 g). ^{1}H NMR ($CDCl_3$) δ ppm 1.48 (m, 2H), 1.55 (m, 1H), 3.34 (dd, J=7,13 Hz, 2H), 3.39 (dd, J=6,13 Hz, 2H), 3.56 (d, J=8 Hz, 2H), 4.50 (s, 2H), 7.32 (m, 5H), ^{13}C NMR ($CDCl_3$) δ (ppm) 138.0, 128.7, 128.1, 73.4, 65.8, 47.6, 19.3, 18.4. IR: 2096. EI HRMS calcd for $C_{13}H_{17}ON_6$ $(M+H)^+$: 273.1464, found: 273.1388.

*4.1.7. ((1R,2S,3S)-3-(Benzyloxymethyl)cyclopropane-1,2-diyl)dimethanamine (**8**).* Triphenylphosphine (0.74 g, 2.84 mmol) was added to a solution of diazide **7** (0.19 g, 0.71 mmol) in dry CH_2Cl_2 (7.1 ml). The mixture was stirred at room temperature under argon for 24 h. Then, water (0.38 ml) was added and the mixture refluxed for 3 h. After the solvent was evaporated, the mixture was purified by flash chromatography (silica, 1:1 CH_2Cl_2/MeOH then 1:1:0.01 CH_2Cl_2/MeOH/NH_4OH). The desired cyclopropyl diamine was obtained as a white solid in 95% yield (0.20 g). ^{1}H NMR ($CDCl_3$) δ ppm 1.17 (m, 2H), 1.30 (m, 1H), 1.81 (br s, 4H), 2.76 (br d, J=7 Hz, 4H), 3.56 (d, J=8 Hz, 2H), 4.50 (s, 2H), 7.31 (m, 5H), ^{13}C NMR ($CDCl_3$) δ (ppm) 138.6, 128.9, 128.2, 128.1, 73.5, 66.8, 37.9, 22.9, 18.5. EI HRMS calcd for $C_{13}H_{21}ON_2$ $(M+H)^+$: 221.1654, found: 221.1654.

4.1.8. (1R,7S*,8S*,Z)-8-(Benzyloxymethyl)-3,5-diazabicyclo[5.1.0]-oct-3-ene (**9**).* Diamine **8** (0.50 g, 2.3 mmol) was dissolved in 20 ml of EtOH. Then, ethyl formimidate hydrochloride (0.25 g, 2.3 mmol) was added and the reaction mixture was stirred under reflux for 10 h. After the solvent was evaporated under vacuum, the residue was purified by flash chromatography (silica, CH_2Cl_2/MeOH 10:1) to give the amidine as a white solid in 88% yield (0.50 g). ^{1}H NMR ($CDCl_3$) δ ppm 1.39 (m, 1H), 1.73 (m, 2H), 3.47 (ddd, J=2,5,14 Hz, 2H), 3.70 (d, J=8 Hz, 2H), 3.93 (dd, J=11, 16 Hz, 2H), 4.48 (s, 2H), 7.27 (m, 5H), 7.49 (s, 1H), ^{13}C NMR ($CDCl_3$) δ (ppm) 154.4, 138.5, 128.4, 127.9, 127.8, 72.8, 65.4, 40.6, 19.7, 17.7. ESI-FTICR (+) calcd for $C_{14}H_{19}ON_2$ $(M+H)^+$: 231.1489, found: 231.1489.

4.1.9. ((1R,7S*,8S*,Z)-8-(Benzyloxymethyl)-3,5-diazabicyclo[5.1.0]-oct-3-en-4-yl)methanol (**11**).* Diamine **8** (0.5 g, 2.5 mmol) was dissolved in 13 ml of EtOH. Then, ethyl 2-hydroxyacetimidate hydrochloride (0.26 g, 2.5 mmol) was added and the reaction mixture was stirred under reflux for 12 h. After the solvent was evaporated under vacuum, the residue was purified by flash chromatography (silica, CH_2Cl_2/MeOH 15:1) to give the hydroxymethyl amidine as a white solid in a 70% yield (0.50 g). ^{1}H NMR (CD_3OD) δ ppm 1.42 (m, 1H), 1.76 (m, 2H), 3.57 (dd, J=6, 14 Hz, 2H), 3.77 (d, J=8 Hz, 2H), 3.95 (dd, J=11, 15 Hz, 2H), 4.19 (s, 2H), 4.53 (s, 2H), 7.33 (m, 5H), ^{13}C NMR ($CDCl_3$) δ (ppm) 166.9, 138.5, 128.5, 128.0, 127.9, 72.9, 65.4, 59.1, 40.3, 19.4, 17.6. ESI-FTICR (+) calcd for $C_{15}H_{21}O_2N_2$ $(M+H)^+$: 261.1598, found: 261.1575.

4.2. General procedure for the deprotection of cyclic amidines

The amidine (1 mmol) is dissolved in 5 ml of freshly distilled MeOH. Ammonium formate (9 mmol) and 0.37 g of 10% Pd/C were added to the solution of amidine. The mixture was refluxed until no more starting material was observed. The suspension was filtered through a Celite pad, which was washed with five portions of MeOH to maximize recovery of the product. The filtrate was concentrated by rotary evaporation. The products were found to be sufficiently pure for use without further purification.

4.2.1. (1R,7S*,8S*,Z)-3,5-Diazabicyclo[5.1.0]oct-3-en-8-ylmethanol (**10**).* This compound was obtained as described in the general procedure for the deprotection of cyclic amidines as a yellowish solid in quantitative yield. ^{1}H NMR (CD_3OD) δ ppm 1.29 (m, 1H), 1.70 (m, 2H), 3.48 (dd, J=6, 10 Hz, 2H), 3.72 (d, J=8 Hz, 2H), 3.92 (d, J=12 Hz, 1H), 3.98 (d, J=12 Hz, 1H), 7.49 (s, 1H), ^{13}C NMR (CD_3OD) δ (ppm) 154.4, 56.9, 40.5, 22.1, 17.6. ESI-FTICR (+) calcd for $C_7H_{13}ON_2$ $(M+H)^+$: 141.1022, found: 141.1024.

4.2.2. (1R,7S*,8S*,Z)-3,5-Diazabicyclo[5.1.0]oct-3-ene-4,8-diyldimethanol (**12**).* This compound was obtained as described above as a white solid in quantitative yield. ^{1}H NMR (CD_3OD) δ ppm 1.24 (m, 1H), 1.65 (m, 2H), 3.52 (dd, J=6, 12 Hz, 2H), 3.74 (d, J=8 Hz, 2H), 3.86 (dd, J=11, 15 Hz, 2H), 4.14 (s, 2H), ^{13}C NMR (CD_3OD) δ (ppm) 166.7, 59.0, 56.9, 40.1, 21.7, 17.5. ESI-FTICR (+) calcd for $C_8H_{15}O_2N_2$ $(M+H)^+$: 171.1128, found: 171.1138.

4.3. Inhibition studies

Initial velocities for enzyme-catalyzed reactions were determined by monitoring absorption at 400 nm due to the appearance of nitrophenol produced during hydrolysis of the corresponding nitrophenyl hexopyranoside. The kinetic assays were performed at 37 °C at pH 6.0 and pH 7.5 using 50 mM Na/citrate/phosphate buffers with the exception of the β-galactosidase from *Escherichia coli* whose buffer contained 10 mM of $MgCl_2$. The glycosidases used were α-galactosidase (green coffee beans), β-galactosidase (*E. coli*), β-galactosidase (*A. orizae*), α-glucosidase (*Saccharomyces cerevisiae*), and β-glucosidase (almonds). The substrate used for each enzyme were the following: *p*-nitrophenyl-α-galactopyranoside (α-galactosidase), *p*-nitrophenyl-α-glucopyranoside (α-glucosidase), *p*-nitrophenyl-β-glucopyranoside (β-glucosidase), and *o*-nitrophenyl-β-galactopyranoside (ONPG) (β-galactosidase). Reaction mixtures were delivered to 1.0 ml quartz cuvettes and allowed to equilibrate to temperature for 3 min prior to addition of enzyme. The reactions were initiated by the addition of the following units and volumes of enzymes: 0.2 U of β-galactosidase (*A. orizae*) in 5 μl for both pHs; 0.2 U of α-galactosidase (green coffee beans) in 10 μl at pH 7.5, and 0.02 U in 15 μl at pH 6.0; 0.1 U of α-glucosidase (*S. cerevisiae*) in 5 μl at pH 7.5 and 0.2 U in 10 μl at pH 6.0; 0.3 U of β-galactosidase (*E. coli*) in 5 μl at pH 7.5 and 0.5 U in 10 μl at pH 6.0; 0.1 U of β-glucosidase (almonds) in 5 μl at pH 7.5 and 0.01 U in 5 μl at pH 6.0. For the inhibition screening assays, the substrate concentration used was around K_m and the amount of enzyme was adjusted to obtain less than 10% hydrolysis of the substrate over 5–10 min reaction time courses. The kinetic parameters (K_m, V_{max}, K_i) were determined using 5–8 substrate concentrations between 0.05 mM and 30 mM, and three different inhibitors concentrations ranging from 0.3 mM to 4 mM. Initial velocity data were fit with non-linear regression directly to the equation for competitive inhibition (Eq. 2) to obtain inhibition constants.

$$v = V_{max} \times [S]/(K_m \times (1 + [I]/K_i) + [S]) \quad (2)$$

Acknowledgements

N.A.H. wishes to thank the National Science Foundation for support of initial phases of this work under MCB0091881. F.M.L.

wishes to acknowledge support via the Reugamer Fellowship. We thank Ms Mirna El Khatib for help recording optical rotations.

Supplementary data

Supplementary data associated with this article can be found in the online version at doi:10.1016/j.tet.2010.05.064.

References and notes

1. Schramm, V. L. *Arch. Biochem. Biophys.* **2005**, *433*, 13–26.
2. Benkovic, S. J.; Hammes, G. G.; Hammes-Schiffer, S. *Biochemistry* **2008**, *47*, 3317–3321.
3. Pauling, L. *Chem. Eng. News* **1946**, *24*, 1375–1377.
4. Wolfenden, R. *Nature* **1969**, *223*, 704–705.
5. Schramm, V. L. *J. Biol. Chem.* **2007**, *282*, 28297–28300.
6. Hiratake, J. *Chem. Rec.* **2005**, *5*, 209–228.
7. Asano, N. *Glycobiology* **2003**, *13*, 93R–104R.
8. Guthrie, R. D.; Jencks, W. P. *Acc. Chem. Res.* **1989**, *22*, 343–349.
9. Demarco, M. L.; Woods, R. J. *Glycobiology* **2008**, *18*, 426–440.
10. Varki, A. *Glycobiology* **2003**, *3*, 97–130.
11. (a) de Melo, E. B.; Gomes, A. D.; Carvalho, I. *Tetrahedron* **2006**, *62*, 10277–10302; (b) Asano, N. *Cell. Mol. Life Sci.* **2009**, *66*, 1479–1492.
12. Vasella, A.; Davies, G. J.; Bohm, M. *Curr. Opin. Chem. Biol.* **2002**, *6*, 619–629.
13. Rye, C. S.; Withers, S. G. *Curr. Opin. Chem. Biol.* **2000**, *4*, 573–580.
14. Yip, V. L. Y.; Withers, S. G. *Biocat. Biotrans.* **2006**, *24*, 167–176.
15. Burgi, H. B.; Dunitz, J. D.; Lehn, J. M.; Wipff, G. *Tetrahedron* **1974**, *30*, 1563–1572.
16. Burgi, H. B.; Dunitz, J. D. *Acc. Chem. Res.* **1983**, *16*, 153–161.
17. Barnes, J. A.; Williams, I. H. *Chem. Commun.* **1996**, 193–194.
18. Horenstein, B. A. In *ACS Symp. Ser. #721*, Truhlar, D., Kniskern, D. P., Morokuma, K., Eds.; American Chemical Society: Washington, DC, 1999; pp 411–423.
19. Lillelund, V. H.; Jensen, H. H.; Liang, X.; Bols, M. *Chem. Rev.* **2002**, *102*, 515–553.
20. Asano, N.; Nash, R. J.; Molyneux, R. J.; Fleet, G. W. J. *Tetrahedron: Asymmetry* **2000**, *11*, 1645–1680.
21. Papandreou, G.; Tong, M. K.; Ganem, B. *J. Am. Chem. Soc.* **1993**, *115*, 11682–11690.
22. Sun, H. B.; Yang, J. S.; Amaral, K. E.; Horenstein, B. A. *Tetrahedron Lett.* **2001**, *42*, 2451–2453.
23. Young, J. E. P.; Horenstein, N. A. *Tetrahedron Lett.* **2004**, *45*, 9505–9507.
24. Dräger, B. *Nat. Prod. Rep.* **2004**, *21*, 211–223.
25. Schmidt, B.; Pohler, M.; Costisella, B. *Tetrahedron* **2002**, *58*, 7951–7958.
26. Collado, I.; Pedregal, C.; Bueno, A. B.; Marcos, A.; Gonzalez, R.; Blanco-Urgoiti, J.; Perez-Castells, J.; Schoepp, D. D.; Wright, R. A.; Johnson, B. G.; Kingston, A. E.; Moher, E. D.; Hoard, D. W.; Griffey, K.; Tizzano, J. P. *J. Med. Chem.* **2004**, *47*, 456–466.
27. Doyle, M. P.; Austin, R. E.; Bailey, A. S.; Dwyer, M. P.; Dyatkin, A. B.; Kalinin, A. V.; Kwan, M. M.; Liras, S.; Oalmann, C. J.; Pieters, R. J.; Protopopova, M. N.; Raab, C. E.; Roos, G. H. P.; Zhou, Q. L.; Martin, S. F. *J. Am. Chem. Soc.* **1995**, *117*, 5763–5775.
28. Evans, D. A.; Woerpel, K. A.; Hinman, M. M.; Faul, M. M. *J. Am. Chem. Soc.* **1991**, *113*, 726–728.
29. Schill, H.; de Meijere, A.; Yufit, D. S. *Org. Lett.* **2007**, *9*, 2617–2620.
30. Faust, J. A.; Mori, A.; Sahyun, M. *J. Am. Chem. Soc.* **1959**, *81*, 2214–2219.
31. Marcelo, F.; He, Y.; Yuzwa, S.; Nieto, L.; Jimenez-Barbero, J.; Sollogoub, M.; Vocadlo, D.; Davies, G.; Bleriot, Y. *J. Am. Chem. Soc.* **2009**, *131*, 5390–5392.
32. Dale, M. P.; Ensley, H. E.; Kern, K.; Sastry, K. A. R.; Byers, L. D. *Biochemistry* **1985**, *24*, 3530–3539.
33. Gloster, T. M.; Meloncelli, P.; Stick, R. V.; Zechel, D.; Vasella, A.; Davies, G. J. *J. Am. Chem. Soc.* **2007**, *129*, 2345–2354.
34. Gloster, T. M.; Davies, G. J. *Org. Biomol. Chem.* **2010**, *8*, 305–320.
35. Ebinger, A.; Heinz, T.; Umbricht, G.; Pfaltz, A. *Tetrahedron* **1998**, *54*, 10469–10480.